ACS OMEGA

http://pubs.acs.org/journal/acsodf

Article

Smart Nanoformulation Based on Stimuli-Responsive Nanogels and Curcumin: Promising Therapy against Colon Cancer

Lizbeth A. Manzanares-Guevara, Angel Licea-Claverie,* Irasema Oroz-Parra, Johanna Bernaldez-Sarabia, Fernando Diaz-Castillo, and Alexei F. Licea-Navarro

Cite This: *ACS Omega* 2020, 5, 9171−9184

Read Online

ACCESS | Metrics & More | Article Recommendations | Supporting Information

ABSTRACT: Curcumin (CUR) has gained much attention for its widely reported anticancer effect; however, its clinical use is restricted due to its low water solubility and, consequently, its poor bioavailability. Here, we report on the use of a nanoformulation of CUR with cationic nanogels for colon cancer therapy. Cationic stimuli-sensitive nanogels were prepared using a scale-up polymerization methodology based on surfactant-free emulsion polymerization of *N*,*N*′-diethylaminoethyl methacrylate (DEAEM) and poly(ethyleneglycol) methacrylate (PEGMA). The obtained nanogels showed a homogeneous size distribution (from 51 to 162 nm, polydispersity index (PDI) < 0.138) and exhibited a spherical form and core−shell morphology as confirmed by dynamic light scattering and electron microscopy, respectively. Nanogels were responsive to and degradable by variations of pH, temperature, or the redox environment, depending on the cross-linker used in the synthesis. Nanogels cross-linked with bis(acryloyl)cystamine incubated in a buffer (pH 7.4) containing 3 mM glutathione degraded in 60 min, while nanogels cross-linked with a divinylacetal cross-linker degraded in 10 min (pH ≤ 6). Nanoformulations of nanogels with CUR were stable as tested up to 30 days at physiological conditions. *In vitro* studies of the human colon cancer cell line (HCT-116) showed a synergistic effect of CUR and the degradable nanogels. Further, *in vivo* acute cytotoxicity tests of empty nanogels in mice demonstrate their potential as CUR nanocarriers for colon-anticancer therapies.

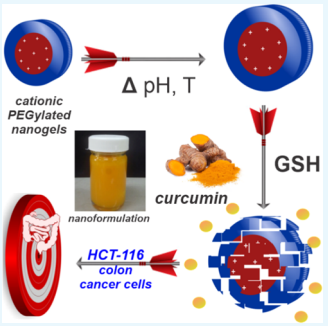

1. INTRODUCTION

Colon cancer, after lung and breast cancer, is the third most common cancer worldwide and is the second cause of cancer-related deaths.[1] For a better patient outcome, it is important to cope with the challenges in cancer treatment. This has led scientists to seek for alternatives to conventional cancer therapies such as surgery, radiotherapy, and chemotherapy.[2] Nowadays, the development of "smart" drug delivery systems (DDSs) based on polymers that are stimuli-responsive, able to release their payload only after "recognition" of pathological tissue modifications, is promising, with a great potential for increasing the efficacy of the treatment.[3] One promising type of DDSs is the so-called nanogels (NGs). NGs are slightly cross-linked polymeric networks of nanometric size with the capacity to hold large amounts of water in their structure. They have a series of tunable properties including flexibility, deformability, dispersibility in biological fluids, stability, and, in some cases, biodegradability. In addition, the NG synthesis is often robust; they swell and shrink in a controlled manner and can be easily loaded with drugs and are able to release them, and many of them have the ability to act as responsive nanocarriers to environmental clues. NGs can be designed as stimuli-responsive materials, which respond to changes in the pH, temperature, reductive environments, activity of enzymes, magnetic field, light, among others.[4−9] This response may cause changes in the conformation of the NGs and can produce an "on-demand" triggered release of any loaded cargo. NG characteristics can be finely regulated by changing their chemical composition.[10] NGs offer several advantages for therapeutic delivery in comparison to existing nanocarriers: (1) a higher storage stability than liposomes and micelles, (2) high drug-loading capacity, (3) controlled drug release, (4) ease of synthesis, and (5) low inherent toxicity.[11,12] In recent years, multiresponsive NGs that respond to a combination of stimuli have been developed in an effort to obtain more effective DDSs. These include multiresponsive biodegradable and cytocompatible nanogels.[13−15] Of the many biological stimuli known, a change in pH is one of the easiest to utilize as a trigger/biological switch.[3] An example of pH-responsive delivery involves the use of amine polymers. Some polymers containing tertiary amines are nonprotonated at pH 7.4, so the polymers are insoluble in water. However, at a lower pH, for instance, at pH 6.5, the tertiary amines become protonated and the polymer becomes soluble in water. NGs prepared using such polymers have been designed for a pH-responsive drug

Received: December 20, 2019
Accepted: April 3, 2020
Published: April 15, 2020

https://dx.doi.org/10.1021/acsomega.9b04390
ACS Omega 2020, 5, 9171−9184

Scheme 1. Synthetic Route for the Formation of PDEAEM-Core-PEG-Shell Nanogels and Their Potential Application in the Development of Smart Nanogels Loaded with Curcumin for Colon Cancer Treatment

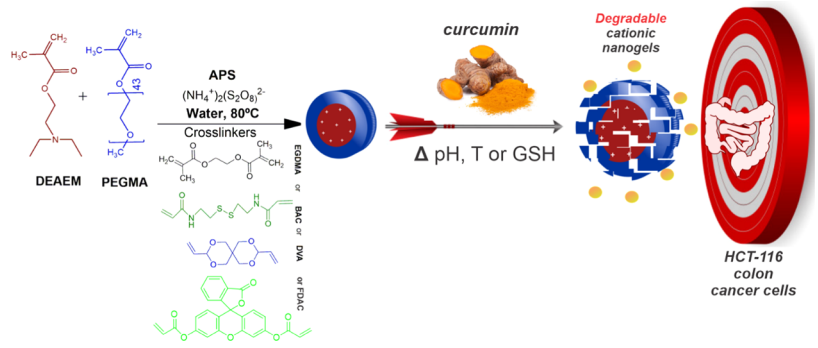

Table 1. General Characteristics of PDEAEM-Core-PEG-Shell Nanogels

key[a]	initiator APS (mol %)[c]	cross-linker (mol %)[c]	DEAEM/PEGMA (weight ratio) feed	D_h (nm)	PDI	ζ-potential (mV)-e-mobil.[d] (μmcm/(V s))	PDEAEM/PEGMA (weight ratio) by ^{1}H NMR[e]
			Nondegradable				
NE1	3	EGDMA (2%)	70:30	162	0.026	+9.62(0.753)	20:80
NE2	3.5	EGDMA (2%)	70:30	140	0.076	+11.4(0.894)	28:72
			GSH Degradable				
NB1	3	BAC (3%)	60:40	65	0.042	+19.8(1.554)	40:60
NB2	2	BAC (2%)	60:40	76	0.002	+18.9(1.483)	36:64
NB3	3	BAC (1%)	50:50	63	0.121	+15.1(1.185)	21:79
NB4	2	BAC (2%)	50:50	65	0.083	+13.6(1.067)	20:80
			Acid Degradable				
ND1	3	DVA (2%)	60:40	52	0.132	+19.5(1.530)	31:69
ND2	2	DVA (2%)	50:50	85	0.080	+20.1(1.577)	34:66
ND3	3	DVA (1%)	50:50	60	0.138	+16.3(1.279)	23:77
ND4	2	DVA (2%)	50:50	51	0.109	+14.2(1.114)	19:81
ND5[b]	3	DVA (1%)	50:50	56	0.107	+13.5(1.059)	17:83
			Fluorescent				
NF1	2	FDAC (1%)	50:50	99	0.066	+18.6(1.460)	19:81

[a]The naming of the nanogels uses N for nanogels; E, B, D, and F for the different cross-linkers used; and a running number; details can be found in Section 4. [b]Prepared with 950 g/mol PEGMA; all other nanogels were prepared with 2000 g/mol PEGMA. [c]mol % with respect to DEAEM. [d]Electrophoretic mobility in parenthesis. [e]The weight ratio does not consider the cross-linker content.

delivery targeted to the decrease in pH in the extratumoral and intracellular microenvironment.[16] Another pH-triggered strategy involves the use of acid-labile functional groups that may cleave at a specific pH, leading to a new hydrophilic chemical entity, or result in the cleavage of a backbone linkage. Such pH-responsive nanocarriers synthesized from polymers containing acid-labile acetal linkages, like the divinylacetal (DVA) cross-linker used in this work, are currently being investigated for drug delivery purposes.[17,18] Another biological switch that can be used for triggered delivery is the difference in glutathione (GSH) concentration in cancer cells (approximately 2−10 mM), compared to that in the normal extracellular matrix (approximately 2−20 μM), thus generating a high redox potential[19] that could serve as a trigger for the selective release of anticancer drugs inside tumor cells. In summary, an ideal stimuli-responsive DDS for chemotherapy should be nanosized, to achieve high tumor accumulation, and should be able to change its structure in response to different environments, to enhance cellular internalization and drug release.[20]

Curcuma longa (turmeric), a spice native to India, contains curcumin (CUR), a natural polyphenolic compound that has the potential to inhibit cancer cell survival, proliferation, invasion, migration, and angiogenesis. CUR has recently gained much attention, especially for its widely reported chemopreventive and/or anticancer activities with minimal side effects.[21−24] These reports include the growth inhibitory performance of curcumin against many tumor cell lines, including bladder, breast, cervical, colon, and prostate cancers.[25−28] However, the clinical use of CUR is restricted by its low water solubility, resulting in poor absorption, following oral administration; consequently, CUR has a poor bioavailability.[29,30] It has been reported that doses as high as 8 g of curcumin per day orally administered to humans resulted only in an average peak serum concentration of 1.77 μM of CUR.[31] CUR nanoformulations are being developed with the goal to overcome its low therapeutic effects.[32,33] Over the past decades, various nanotechnology-based systems, such as cyclodextrin complexes, dendrimers, gold nanoparticles, liposomes, magnetic nanoparticles, micelles, nanoemulsions, polymeric nanoparticles, and solid lipid nanoparticles, have been being explored in the pursuit to improve the aqueous solubility of curcumin and drug delivery to the pathological site;[34,35] however, for a nanogel-based approach, there is only one report in the literature aiming at treating colon cancer.[36] In that study, a gelatin polymer and an acrylamide glycolic acid (AGA) monomer were reacted to form anionic interpenetrating polymeric network nanogels (IPN-NGs) through a simple

https://dx.doi.org/10.1021/acsomega.9b04390
ACS Omega 2020, 5, 9171−9184

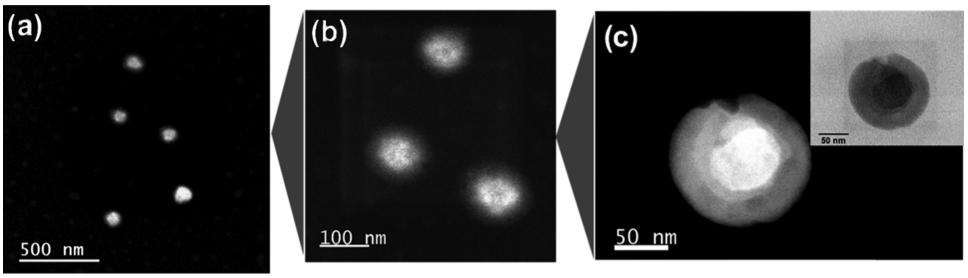

Figure 1. TEM micrographs of PDEAEM-core-PEG-shell nanogels cross-linked with EGDMA (NE2) stained with phosphotungstic acid: (a−c) NE2 nanogels at different magnifications (dark field and bright field for the highest magnification).

emulsion polymerization methodology for the encapsulation of CUR. Interestingly, CUR-loaded NGs released CUR to a greater extent at pH 7.4 than at pH 1.2 *in vitro*, suggesting that these nanogels exhibit pH-sensitive properties that could be exploited in oral delivery.[36]

In the present contribution, a nanoformulation of CUR loaded on well-defined PDEAEM-core-PEG-shell nanogels was formulated, aiming at intravenous injection for colon cancer delivery. PDEAEM nanogels are not ionized at pH 7.4 and start ionizing at pH values below 7, so the CUR delivery is expected at the tumor site (pH 6.8) or inside cells (endosomal pH 6−5). Modifications in the synthesis of nanogels were explored; for example, different cross-linkers were tested to obtain pH- and GSH-degradable nanogels, in addition to pH and temperature responsiveness provided by PDEAEM nanogels, resulting in DDSs with different physicochemical properties. It is worth mentioning that this formulation based on PDEAEM−PEG−cationic nanogels and curcumin is reported in the literature for the first time.

2. RESULTS AND DISCUSSION

2.1. Synthesis and Characterization of Nanogels. The synthetic protocol followed is pictured in Scheme 1. Polymerizable PEG methyl ether methacrylate (PEGMA) (2000 g/mol) stabilizes water-insoluble DEAEM (at neutral pH) in a micellar-type construct that is polymerized with the addition of the free-radical initiator and is stabilized with the cross-linker added, to yield a series of core−shell nanogels of different physicochemical properties presented in Table 1. The yield of all reactions was close to 30 wt %, a yield that may be improved in the future by controlling the pH of the polymerization system; nevertheless, about 2 g of purified nanogels was obtained per reaction. It was found that the characteristics of these nanogels are preserved after scaling the synthesis (16 times the small scale reported previously), so it was possible to obtain reproducible and scalable nanogels (Figure S1 in the Supporting Information (SI)). It is worth mentioning that one of the current challenges for drug delivery systems is precisely the aspect of large-scale production and maintaining the size and composition of nanocarriers at large scale. That is why currently only a limited number of nanocarriers have been introduced into clinical trials. There is a great development of nanosystems with high potential, but they are limited because they are not scalable. There is always a need to scale up laboratories or pilot technologies to increase their potential and facilitate their eventual application.[37] Predesigned nanogels can be obtained by this surfactant-free emulsion methodology, and the size, composition, physical properties (surface charge), and chemical properties (solubility) can be controlled by varying the reaction parameters. An important aspect to consider was the molecular weight (MW) of the PEGMA used as a stabilizer during the synthesis. It has been reported that the MW of the PEG used in PEGylation of nanoparticles affects the toxicity of these particles because it is known to avoid the process of opsonization, which is one of the most important biological barriers to controlled drug delivery. Opsonin proteins present in the blood serum bind to nonstealth nanoparticles, allowing macrophages of the mononuclear phagocytic system (MPS) to easily recognize and remove them. Several methods have been developed to mask or camouflage nanoparticles from the MPS. One is the adsorption or grafting of poly(ethylene glycol) (PEG) to the surface of nanoparticles.

This method creates a hydrophilic protective layer around the nanoparticles that is able to repel the absorption of opsonin proteins via steric repulsion forces, thereby blocking and delaying the first step in the opsonization process.[38] Most research indicates that a surface PEG chain molecular weight of 2000 g/mol or greater is required to achieve increased MPS avoidance characteristics. This minimum MW is most likely due to the loss in the flexibility of shorter PEG chains.[38] Therefore, for this report, we made an important modification by including PEGMA MW = 2000 in the preparation of PDEAEM nanogels, whereas in previous reports of our group, mainly PEGMA MW = 1100 was used.[39] The PDEAEM nanogels with a PEGMA MW = 2000 shell were obtained effectively at the half of the initial concentration of reactants used for the synthesis of PDEAEM nanogels with a PEGMA MW = 1100 shell, which may be due to the steric effect impaired by the PEG itself.[38]

Nanogels with varying PDEAEM content (17−40 wt %) and PEGMA content (60−83 wt %), with sizes between 51 and 162 nm (hydrodynamic diameter, D_h), were obtained depending on the cross-linker type and its concentration. Using BAC and DVA as cross-linking agents, smaller nanogels (less than 85 nm) were obtained than using the ethylene glycol dimethacrylate (EGDMA) cross-linker, and this may be related to its solubility in aqueous medium, since EGDMA is more soluble in water than DVA and BAC.[40,41] All nanogels show positive surface charge (ζ-potential) at pH values less than 7.4. Prepared nanogels showed unimodal and narrow distributions with polydispersity index (PDI) < 0.138 (Figure S2 in SI). All of these features preclude their good performance as drug delivery systems. The chemical composition of the nanogels was determined by ^{1}H NMR (Table 1) and shows in general terms that DEAEM was incorporated in a lower amount than in the feed, similar to the previous report using PEGMA with MW = 1100 g/mol.[39] The spectra (^{1}H NMR) of the nanogels, together with a detailed description of signals and composition calculations, can be found in the Supporting Information

https://dx.doi.org/10.1021/acsomega.9b04390
ACS Omega 2020, 5, 9171−9184

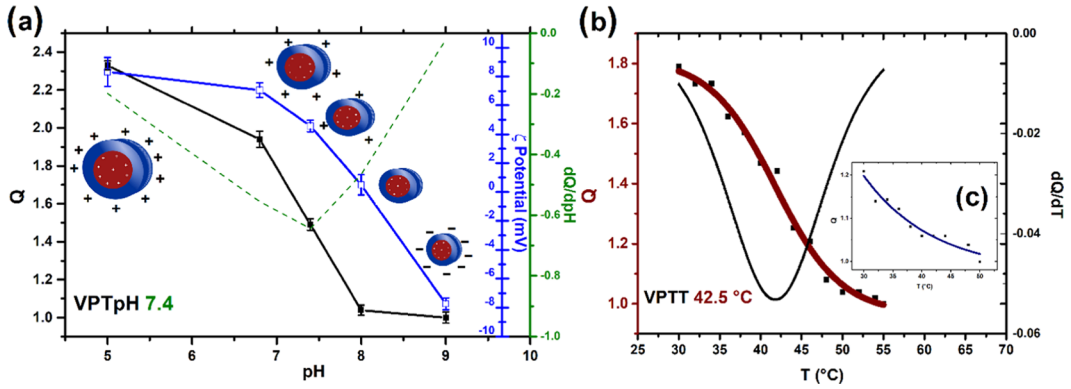

Figure 2. Responsive behavior of PDEAEM-core-PEG-shell nanogels (NE2, cross-linked with EGDMA): (a) Swelling ratio (Q) and ζ-potential as a function of pH. Q as a function of temperature (b) at pH 6.8 and (c, inset) at pH 7.4.

(Figures S3−S6 in SI). More insights into the characteristics of these types of core−shell nanogels were reported earlier elsewhere.[39]

An important characterization tool for nanoscopic materials is microscopy. For the nanogel characterization, two different microscopic techniques were employed: atomic force microscopy (AFM) and transmission electron microscopy (TEM). The characterization by AFM was used to show the morphology and to confirm the size of the nanogels (Figure S7−S9 in SI), while the core−shell structure was evidenced by TEM. Nanogels were treated with a phosphotungstic acid solution to stain the nucleus of PDEAEM.

Figure 1 shows the TEM images of nondegradable nanogel particles: PDEAEM/PEGMA (28:72)/EGDMA$_{2\%}$ (D_h: 140 nm). In the case of degradable nanogels, the staining agent with acidic chemical nature could not be used.

2.2. pH and Temperature Sensitivity of PDEAEM-Core-PEG-Shell Nanogels. Of the many biological stimuli known, a change in pH is one of the most prevalent and easiest to utilize as a trigger or biological switch. Compared to the neutral pH found in many healthy tissues (pH 7.4), the presence of ischemia or tumor cells in the nearby tissue is signaled by a decrease in pH (pH 6.5−7.2); furthermore, entrance into a cell via endocytosis is accompanied by acidic conditions (the endosomal pH is 5−6.5). One strategy for developing responsive polymers is to take advantage of the changes in polymer protonation states that occur with changes in the pH. Such a change can transform an insoluble or hydrophobic polymer into a hydrophilic and completely water-soluble polymer, which will then readily release and deliver its payload/drug.[3] The possible application of PDEAEM nanogels relies on their pH sensitivity, and recently, it was reported that they also show temperature-responsive behavior at pH values close to the physiological pH.[42] Through the synthesis route used in this study, a slightly cross-linked core of PDEAEM is expected to be formed with PEG-tethered chains. PDEAEM is a hydrophobic polymer at neutral pH but possesses tertiary amine groups in each repeating unit, and it can be ionized by acids, yielding a hydrophilic polymer.[39] Figure 2a shows plots of swelling ratio (Q), as determined by dynamic light scattering (DLS) measurements, for a PDEAEM/PEGMA (28:72)/EGDMA$_{2\%mol}$ nanogel (NE2) as an example of its ability to respond to a pH change. This nanogel exhibited an increase of 120% in volume by passing from pH 8 to pH 5, and the ζ-potential values increased due to the increase in the degree of ionization of PDEAM with a pH decrease in the medium. The pH-responsive behavior is similar to that of other PDEAEM-based nanogels reported in the literature.[42−44] The pH-responsive behavior of other synthesized nanogels can be found in SI, Figure S10, while the pH-responsive behavior of DVA- and BAC-cross-linked nanogels is not reported since they degrade in acidic conditions. All of the nanogels presented a volume phase transition pH (VPTpH) at around pH 7.4. Below that VPTpH, nanogel particles were swollen, and above it, particles were shrunken, reducing their size due to the deprotonation of amine groups of PDEAEM and the weakened electrostatic repulsion. The ζ-potential values were fully consistent with the expected behavior of the nanogels and corroborate the cationic nature of PDEAEM at pH values of biological interest.

For the temperature sensitivity, the measurements were based on their swelling ratio (Q) at each temperature, taking the highest measured temperature as the collapsed state, under certain pH conditions. Figure 2b,c (inset) shows this study; the PDEAEM-core-PEG-shell nanogel (NE2) at pH 6.8 shows a clear trend of decreasing Q by heating from 1.8 at 30 °C to 1 at 55 °C, equivalent to a shrinkage of 80% relative to the volume at room temperature.

The derivative of size with respect to temperature shows that the phase transition temperature (VPTT) is occurring at an average value of 42.5 °C (pH 6.8). When the pH value is 7.4, the same nanogel also shows a tendency of decreasing Q by heating, going from 1.2 to 1, which reflects a shrinkage of 20% as compared to its volume at 30 °C. The VPTT cannot be clearly determined at this pH, but it seems to be close to ∼36 °C. At pH 5, there was no temperature-responsive behavior observed up to 55 °C. An explanation for this behavior can be found if we take into account that with decreasing pH a higher ionization degree of the tertiary amines is observed, allowing more water molecules to solvate the charged groups; therefore, a larger number of hydrogen bonds need to break (higher temperature) to induce a shrinkage of the nanogels.[40] The temperature-responsive behavior of other synthesized nanogels can be found in SI, Figure S11.

A thermal responsive behavior, in addition to the response to pH variations, makes these nanogels more suitable for bioapplications since they respond to two stimuli.

Finally, using a fluorescent cross-linker, a PDEAEM-based nanogel was synthesized to use it in cell-internalization studies. The resulting nanogel exhibited green fluorescence, and its general physical and chemical characteristics are shown in

https://dx.doi.org/10.1021/acsomega.9b04390
ACS Omega 2020, 5, 9171−9184

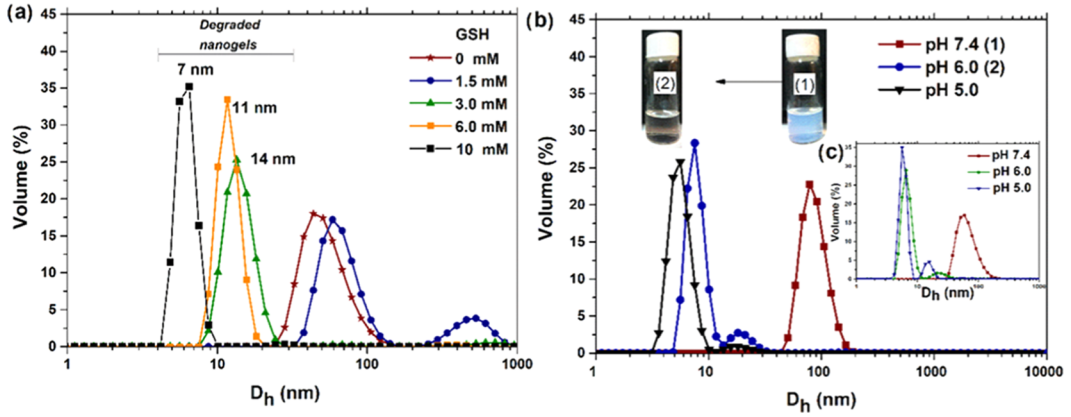

Figure 3. Degradation studies of PDEAEM-core-PEG-shell nanogels by DLS: (a) size distributions of nanogels cross-linked with BAC (NB2) at different concentrations of GSH, (b) size distributions of nanogels cross-linked with DVA (ND2) at different pH values, and (c) size distributions of nanogels cross-linked with BAC (NB2) at different pH values (inset). (The photographs were taken by the authors of the manuscript.).

Table 1. More insights into the characteristics of these nanogels are the subject of future studies.

2.3. GSH and Acid Degradation of PDEAEM-Core-PEG-Shell Nanogels. In recent years, nanogels releasing therapeutics in response to an intracellular redox potential have attracted great interest; they are advantageous over conventional drug delivery carriers. The basic principle for the preparation of these systems is the incorporation of redox-active units such as disulfide bonds and cleavage of these linkages in the presence of reducing agents, for example, GSH.[45] In this work, PDEAEM-core-PEG-shell nanogels were provided with a redox-responsive cross-linker containing cystamine (BAC) as a redox-responsive constituent, forming three-dimensional (3D) cross-linked redox-responsive networks to hold the therapeutics and to be able to break the networks in response to a redox trigger to release the payload under biodegradation conditions. The redox-sensitive property of the polymeric nanogels was investigated via DLS by monitoring particle size change with the varying concentrations of GSH from 1.5 to 10 mM at pH 7.2 (37 °C). The results show that the nanogels were rapidly destabilized by GSH in 0.5 h and further degraded into small aggregates depending on GSH concentration (Figure 3a). It was reported in the literature that hydrophilic nanogels disassociated rapidly when incubated in reduction conditions, while nanogels composed of amphiphilic components would form agglomerates first;[46] this was observed in the current study at a GSH concentration of 1.5 mM. A similar behavior was recently reported for poly(*N*-vinylpyrrolidone-*co*-*N*-vinylformamide) copolymer-based nanogels cross-linked with a disulfide-based PEG diacrylate cross-linker.[47] The nanogels were degraded in 1 h of exposure to 10 mM GSH. The authors studied the effect of the cross-linking density on drug release rate and degradation behavior, where nanogels synthesized with a higher cross-linking density (15%) showed a slow drug release and slower degradation than at a cross-link density of 5%. In the current report, the PDEAEM-core-PEG-shell nanogels were cross-linked using a smaller amount of BAC (2%); therefore, the rapid degradation observed is not a surprise. Increasing the cross-linking density may be an opportunity to modulate the degradation of nanogels, depending on the application requirements, which can be undertaken in future studies. The nanogels cross-linked with BAC exhibited good GSH-responsive degradation behavior, showing 100% of degradation to smaller particles in the presence of 3 mM and higher GSH within 0.5 h. The other nanogels prepared (cross-linked with EGDMA, DVA, and fluorescein diacrylate (FDAC)) did not show degradation at the same conditions (up to 10 mM GSH) until 24 h (Figure S12, SI). Presumably, the degradation of the developed BAC-cross-linked PDEAEM/PEG nanogel systems could be efficient under intracellular-mimicking reducing conditions. Further, degradation and solubilization of PEG-based redox-responsive nanogels in the reducing environment of cytosol provide an excellent opportunity to deliver the drug at the site of action.[45]

On the other hand, based on the effort to obtain more effective DDSs, multiresponsive nanogels, which respond to a combination of two or more stimuli but also degrade in response to a stimulus, are sought. The use of an acid-labile acetal cross-linker (DVA) is an alternative, since it has the potential to decrease the effects caused by the accumulation of nanocarriers in the body. The acid-medium-sensitive property of the PDEAEM-core-PEG-shell nanogel cross-linked with DVA (ND2) was tested by changing the pH of the dialyzed nanogel dispersion abruptly from 7.4 to 6.0.

Results are shown in Figure 3b, and the proposed degradation mechanism is shown in Figure S13 (SI). A macroscopic hint that degradation has occurred can be seen in the color change of the nanogel dispersion that turned from a cloudy to a clear solution. Dynamic light scattering (DLS) measurements demonstrated that the average size decreased from ∼85 nm to close to 8 nm in a bimodal distribution. Under the same conditions, the nanogels cross-linked with BAC (NB2) were also degraded (see Figure 3c, inset). By testing the effect of a change in pH from 7.4 to 5, similar degradation behavior was observed; only slightly smaller sizes were obtained. It should be noted that the pH- and redox-responsive nanogels maintain superior stability in normal physiological conditions (pH 7.4, 37 °C).

2.4. Stability of PDEAEM-Core-PEG-Shell Nanogels. PEGylation of a nanogel is an essential process of decorating the particle surface by covalent grafts of the PEG chains[44] and provides stability under physiological conditions. Improved dispersion stability is another added advantage, to avoid aggregation behavior, commonly encountered during the preparation and storage of nanogels or even upon intravenous injection. Selected nanogels (NE2, NB3, ND4, and NF1) were studied at pH 7.4 (37 °C) for 48 h. The evolution of the

https://dx.doi.org/10.1021/acsomega.9b04390
ACS Omega 2020, 5, 9171−9184

hydrodynamic diameter (D_h) was monitored by DLS. The hydrodynamic diameter of the different nanogels was maintained to sizes very similar to the size in the zero time, indicating good stability of the particles under these conditions (Figure S14, SI). The stability was also evaluated for selected PDEAEM-core-PEG-shell nanogels at 37 °C in biological mimicking media: concentration: 25 μg/mL, cell culture medium (RPMI-1640) supplemented with 10% fetal bovine serum (FBS). In Figure S15 (SI), the hydrodynamic diameter evolutions of NE2, ND5, and NB4 are shown. The nondegradable nanogels (NE2, cross-linked with EGDMA) increase their D_h gradually as the incubation time increases. What is happening? Nanogels have a slightly positive charge at a pH of 7.4, while the ζ-potential of BSA in the supplemented culture medium (RPMI-1640) was −8.4 mV, indicating that BSA is negatively charged at pH 7.4 (Figure S16, SI). Therefore, BSA could be adsorbed onto the nanogel surface by electrostatic attraction, increasing the sizes of nanogels from 140 to 400 nm. Similar behavior was reported for cationic poly(tri(ethylene glycol) methyl ether methacrylate)-*b*-poly-(pentafluorophenyl methacrylate)-based nanohydrogel particles in the presence of BSA.[48] The authors reported that after incubation for 30 min positively charged nanohydrogel particles with negatively charged BSA aggregates were formed, owing to the adsorption of BSA. However, in the case of the degradable nanogels NB4 (cross-linked with BAC) and ND5 (cross-linked with DVA), the D_h decreased after 1 h of the incubation to values close to 10 nm, showing evidence of their degradation due to some interaction with any of the multicomponents of the supplemented culture medium.

Finally, the storage stability of the empty nanogels (NE2, cross-linked with EGDMA) was evaluated at room temperature (25 °C) and monitored by DLS. Their integrity was verified at storage conditions, and surprisingly, they remain almost intact for 18 months under the conditions described in the methodology (Figure S17, SI). For nanogels cross-linked with BAC and DVA, preliminary results showed stability for nondialyzed solutions (25 °C) for at least 4 months after their preparation without aggregation (Figure S18, SI).

2.5. CUR Loading and *In Vitro* Release from the PDEAEM-Core-PEG-Shell Nanogels. In contrast to other nanomaterials, polymeric nanogels have the best combination of properties for the development of potential drug delivery carriers.[6] The most important aspect is the ability of nanogels to exhibit a response to different stimuli, in this case, pH, temperature, and GSH presence, to achieve a triggered release of the drug at the target site. Selected nanogels were loaded with CUR, following the procedure described in the Section 4, and then quantified using a calibration curve shown in Figure S19 (SI). The results of the CUR loading content (DLC) were from 15 to 6 wt %, depending on the cross-linker used for the nanogel synthesis (Table 2). For NE2 (cross-linked with EGDMA), it was the highest, and for ND3 (cross-linked with DVA), it was the lowest. Similar values of DLC were reported in the literature for CUR in other types of nanocarriers.[49−51] Interactions between CUR and the nanogels are expected to occur through hydrogen bonding as shown in Figure 4. The magnitude of the surface charge was very slightly attenuated for all nanogels when the CUR was added (ζ-potential values, Table 2), and only in the case of the ND3 nanogel, this value decreases compared to the neat nanogels. It is possible that in the latter case CUR is not only contained in the nanogel core but also adsorbed on the nanogel surface.

Table 2. General Characteristics of CUR-Loaded PDEAEM-Core-PEG-Shell Nanogels

key	D_h (nm)	ζ-potential (mV)	DLC (%)	DLE (%)
NE2 + CUR	230	+22.6	15.75	28
NB4 + CUR	187	+13.3	7.44	13
ND3 + CUR	290	+9.62	5.58	12

Since curcumin is poorly soluble in water at acidic or neutral pH, the macroscopic undissolved flakes are visible in the solution (Figure 4a, picture), while the aqueous dispersion of the curcumin-loaded nanogels is homogeneous, with its hue derived from the natural color of curcumin (Figure 4c,d,e). The morphology of the CUR-loaded nanogels (ND3) at normal physiological conditions (pH 7.4) was analyzed by field emission scanning electron microscopy (FESEM). From the image (Figure S20, SI), it is clear that the CUR-loaded nanogels show spherical morphology but their size varies with the loading process, to be larger than that of the empty nanogels. Particles were observed from 200 nm up to 500 nm in comparison to 51 nm (see Tables 1 and 2), demonstrating aggregation caused by CUR loading in nanogels. Since CUR is a fluorescent molecule, its application in drug delivery to cells can be followed by its intrinsic fluorescence. In Figure S21 (SI), there are some images evidencing the green fluorescence of the CUR-loaded nanogels.

The stability of the curcumin-loaded nanogels (NE2, cross-linked with EGDMA) was evaluated at 37 °C in the dark by DLS analysis from day 1 to 30 days after preparation. Results shown in Figure S22 (SI) evidence that the size change was less than 28% (comparing day 1 and day 30), with a slight increase in the dispersity (PDI) from 0.090 to 0.203.

The physical appearance of these CUR-loaded nanogel dispersions is shown in Figure 4. Their stability is superior to the stability of easily disassembling micellar systems and other drug delivery systems.

CUR drug release experiments from CUR-loaded nanogels were carried out *in vitro*. The percentages of CUR released from three types of nanogels under different conditions are shown in Figure 5.

In a phosphate-buffered saline (PBS) solution at pH 7.4, the free CUR drug diffuses very slowly from the dialysis bag because of the low water solubility, reaching less than 6% cumulative release after 220 h (∼9 days). CUR also does not diffuse faster at pH 5. However, when CUR is loaded in the nanogels, the release rate is faster when a nondegradable nanogel is used (NE2). The cumulative release of CUR increases at pH 7.4 to ∼10%, but, most importantly, at pH 5, the cumulative release is 32%, with a linear increase up to 160 h. This is a result of the swelling of the nanogels related to the ionization of DEAEM units at pH 5. When CUR is loaded in the ND3 nanogel, which is acid degradable, the cumulative release of CUR goes up to 60% at pH 5 in 70 h, which is attractive since it mimics the conditions in cell endosomes.

In the case of the NB4 nanogels, which combine pH sensitivity, acid degradability, and GSH degradation, the CUR release rate is accelerated at pH 5 (20% in 48 h) and even more in the presence of GSH (45% in 48 h). After 60 h, the cumulative CUR release reaches 80% in the presence of 10 mM GSH and pH 5. The significantly enhanced release is mainly due to the efficient cleavage of the cross-linking network of nanogels NB4 (cross-linked with BAC). These

https://dx.doi.org/10.1021/acsomega.9b04390
ACS Omega 2020, 5, 9171−9184

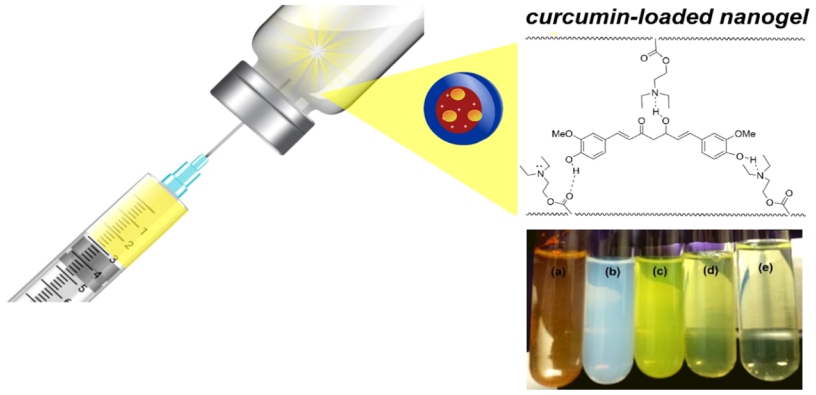

Figure 4. Smart nanoformulations based on stimuli-responsive PDEAEM-core-PEG-shell nanogels and curcumin (1 mg/mL). (a) Free CUR in aqueous media, (b) dispersion of empty nanogels, (c) CUR-loaded nanogels (NE2), (d) CUR-loaded nanogels (NB4), and (e) CUR-loaded nanogels (ND3). (Photographs were taken by the authors of the manuscript; other elements are free domain).

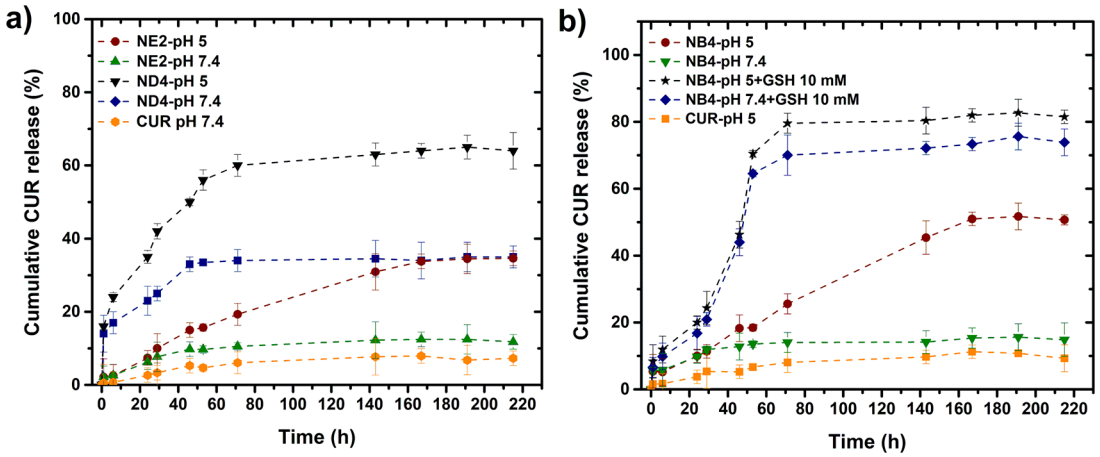

Figure 5. Cumulative drug release of curcumin at pH 7.4 and 5 (37 °C): (a) from NE2 (EGDMA cross-linked) and ND3 (DVA cross-linked) and (b) NB4 (BAC cross-linked).

results suggest that CUR nanogel formulations are quite stable at physiological conditions, and the triggered drug release by intracellular-mimicking reduction conditions (10 mM GSH) proceeds in a sustained manner up to 70 h for NB4. This system exhibits faster release under a higher GSH concentration and a lower pH; the phenomenon was described to be due to conditions of simultaneous cleavage of disulfide linkages and ionization of amino groups. For the nanogels cross-linked with DVA, a burst in the release was observed before 10 h, followed by a sustained release up to 40 h (pH 7.4) and 70 h (pH 5); a combination of swelling and degradation is responsible for this behavior. The availability of CUR in aqueous conditions is enhanced using nanogel formulations, while the release rate could be controlled via the selection of the cross-linker type and medium conditions.

2.6. *In Vitro* Therapeutic Efficacy. The anticancer activity of free CUR against the human colon cancer cell line HCT-116 was examined using the cell proliferation 3-(4,5-dimethylthiazol-2-yl)-2,5-diphenyltetrazolium bromide (MTT) assay after incubation for 24 h at 37 °C, pH 7.4, and 5% CO_2. It is worth mentioning that this test is preferable over MTS to avoid the interference of curcumin absorbance with the MTS reagent. Cell viability in the presence of the empty nanogels was also examined since it is reported that PDEAEM-containing nanogels show cytotoxicity depending on their concentration.[46] Nondegradable nanogels, cross-linked with EGDMA (NE2), were found to be nontoxic up to 400 μg/mL concentration. This indicates the biocompatibility for the cell line HCT-116 as shown in Figure S23a (SI). This type of nanogel was the largest tested nanogel (140 nm) with a lower positive ζ-potential (+11.4 mV). According to the hypothesis named "wrapping time" of the membrane, nanocarriers with large size need a stronger driving force and additional energy for a cellular internalization process; therefore, cellular uptake decreases with the augmentation of the particle size of nanogels.[52] Additionally, the higher positive surface charge leads to a stronger affinity for the negatively charged cell membrane, accounting for its higher cellular uptake.[53] An example can be seen with nanogels cross-linked with DVA (SI, Figure S24). ND3 nanogels showed a tendency of greater size and cross-linking density and less cytotoxicity. The degradable nanogels NB4 (cross-linked with BAC, D_h 65 nm, ζ-potential +13.6 mV) and ND3 (cross-linked with DVA, D_h 65 nm, ζ-potential +16.3 mV) resulted in being cytotoxic for the HCT-116 cell line with IC_{50} values of 80 and 65 μg/mL, respectively. This is not a big surprise because in the studies of degradation in RPMI-1640 medium described before, these same nanogels showed some degradation after 1 h, which can leave exposed the cationic PDEAEM segments in the core with the capacity to interact with the cell membrane, leading to cell internalization; the last aspect has been shown by several investigations.[54−56] Is this factor

https://dx.doi.org/10.1021/acsomega.9b04390
ACS Omega 2020, 5, 9171−9184

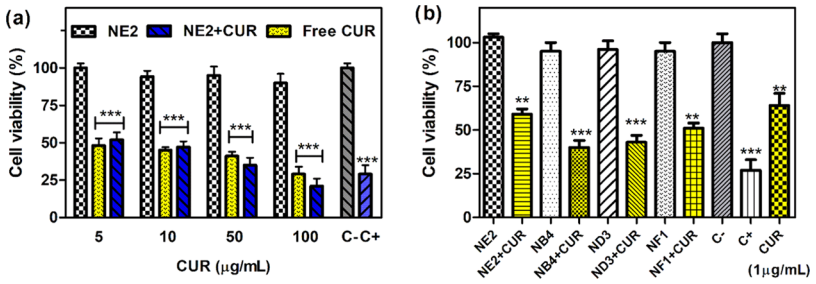

Figure 6. Cytotoxic effects of empty PDEAEM-core-PEG-shell nanogels, CUR-loaded nanogels, and free CUR on the human colon cancer cell line HCT-116. Cytotoxicity of (a) nondegradable nanogels (NE2, EGDMA cross-linked), CUR loaded NE nanogels (blue) and free CUR (yellow) at different CUR concentrations; and (b) CUR-loaded nondegradable nanogels (NE2, EGDMA cross-linked), CUR-loaded GSH-degradable nanogels (NB4, BAC cross-linked), and CUR-loaded degradable nanogels (ND3, DVA cross-linked) at an equivalent 1 μg/mL CUR concentration. The cell viability (%) of cells is expressed as a function of untreated cells (C−). The results represent the average ± standard error of the mean (SEM) of triplicates. Positive control (C+) 5% dimethyl sulfoxide (DMSO). $p < 0.05$, $^{**}p < 0.01$, $^{***}p < 0.001$, and $^{****}p < 0.0001$ vs C− (unpaired Student's *t*-test).

positive or negative? It is positive if the nanocarrier becomes a nanodrug against cancer after cell internalization, improving the activity of the loaded drug. Cell viability experiments were carried out in a human colon cancer cell line using nondegradable (NE2) and degradable (NB4 and ND3) nanogels below the concentrations that already cause cytotoxicity. Interestingly, when the CUR-loaded degradable nanogels were studied (NB4 and ND3), cell viability was reduced below 50%, which is more cytotoxic than free CUR (1 μg/mL) at the same equivalent concentration of CUR (Figure 6b). In the case of the nondegradable nanogels (NE2 cross-linked with EGDMA), a higher concentration of CUR was needed to achieve 50% of cell viability (CUR = 5 μg/mL, see Figure 6a).

Free curcumin shows that the IC_{50} for this cell line is 5 μg/mL (see also SI, Figure S25), so a dosage of 1 μg/mL CUR inside degradable nanogels to achieve 50% viability is a clear indication of a synergistic effect of CUR nanogels. Fluorescence microscopy images of cells stained with propidium iodide (PI) and treated with CUR-loaded ND3 support this conclusion (see Figure 7). When CUR was loaded in nondegradable nanogels (NE2 cross-linked with EGDMA) and a dosage of 1 μg/mL CUR equivalent was used, which is one-fifth of the IC_{50}, fluorescence microscopy showed not only many viable cells but also some deformed cells (SI, Figure S26). Interestingly, curcumin is present inside the cells, demonstrating that NE2 delivered it inside cells, and presumptively, its accumulation produces cell death. The question arises, Are the nanocarriers internalized inside cells? Or does the nanocarrier deliver CUR in the proximity of the cell membrane? This result suggests that it can be a synergistic effect between the degradable nanogels and curcumin. Fluorescent PDEAEM-core-PEG-shell nanogels were synthesized to study cell internalization in more detail, replacing the EGDMA cross-linker with a fluorescent one, FDAC, resulting in nanogels with green fluorescence. These nanogels are denoted NF1 in Table 1. Cellular internalization studies were performed by varying treatment times from 5, 15, 30, 45, 60, 90, 120, 180 to 240 min and the concentration of nanogels from 50 to 400 μg/mL in HCT-116 cells. The internalization rate of these nanogels is very fast; only viable cells were found at the shortest times of treatment (5, 15, and 30 min) at a concentration of nanogels of 100 μg/mL, giving substantial evidence demonstrating cellular internalization similar to that reported in the literature for other PDEAEM nanocarriers.[54−56] Cell nuclei were counterstained with Hoechst 33258 in blue, and the fluorescent nanogels (NF1) can be visualized in green. Fluorescent nanogels were preferably located outside of the cells until 15 min, and they were accumulated in the cell membrane; however, these nanogels were observed in the interior of the cells at 30 min (Figure 8).

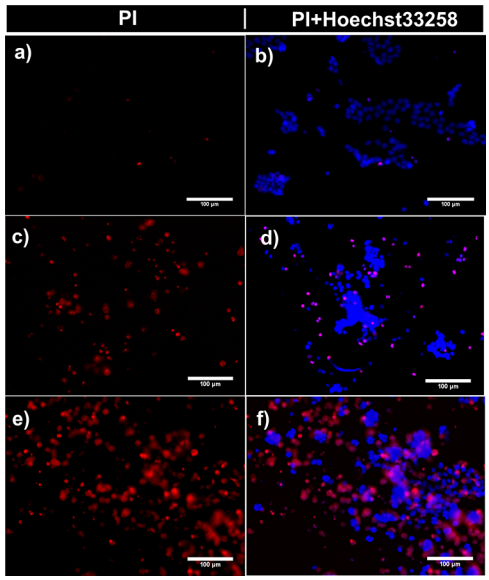

Figure 7. Fluorescence microscopy images of the human colon cancer cell line (HCT-116): (a, b) cells incubated for 24 h with empty PDEAEM-core-PEG-shell nanogels NE2 (cross-linked with EGDMA), (c, d) cells incubated with CUR-loaded nanogels ND3 (cross-linked with DVA) for 3 h, and (e, f) cells incubated with CUR-loaded nanogels ND3 for 24 h. Representative images show cells treated with propidium iodide (PI), which is used to identify necrotic or apoptotic cells (red), and cell nuclei were counterstained with Hoechst 33258 in blue.

2.7. *In Vivo* Studies. Very few nanogels have been evaluated *in vivo*. In this scenario, we begin to assess the acute toxicity of empty nanogels, taking as an example a nondegradable (NE2) and a GSH-degradable (NB4) system; results are described in Table 3. After five days of acclimatization, each group of mice was exposed to one of the two nanogel compounds. The result of the administration of nanogels in different doses was the same for both compounds, resulting in the survival of the mice at all of the doses tested. However, the animals showed symptoms of pain

https://dx.doi.org/10.1021/acsomega.9b04390
ACS Omega 2020, 5, 9171−9184

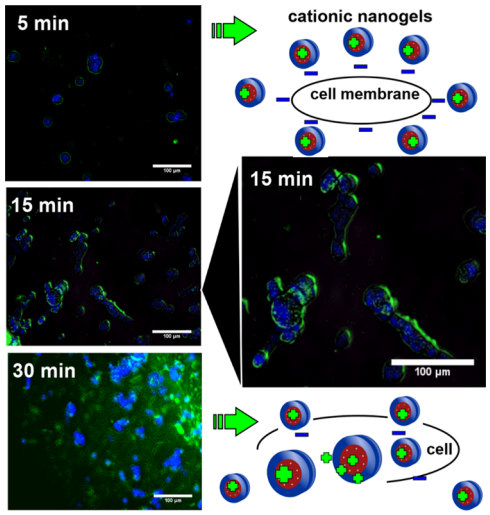

Figure 8. Cell-internalization images using fluorescence microscopy of fluorescent PDEAEM-core-PEG-shell nanogels (100 μg/mL for 5, 15, and 30 min of incubation); cell nuclei were counterstained with Hoechst 33258 in blue, and fluorescent nanogels (NF1) were visualized in green.

Table 3. Effect of Different Doses of NB4 and NE2 by the Intraperitoneal Route on the Survival of Mice during 48 h[a]

dose (mg/kg)	log dose	NB4 score	NE2 score
10	1.00	O	O
20	1.30	O	O
40	1.60	OOO	OOO

[a]"O" indicates survival, and "X" indicates death.

during the first hour after the nanogel injection, such as passive behavior, arching, and difficulty to move, but all animals recovered without any visible sequels. As specified by the OECD protocol,[57] under some circumstances, statistical computation will not be possible. One of these special conditions to determine and report the LD_{50} is the criteria for stopping the experiment when the upper limit is repeatedly tested without a lethal effect.

Therefore, the final score was "OOOOO", and the LD_{50} by the intraperitoneal route was higher than 40 mg/kg for NB4 and NE2 nanogels, despite the differences in degradability. More *in vivo* studies are currently under investigation in our research group using these nanogels.

3. CONCLUSIONS

Smart polymeric nanogels containing stimuli-responsive units in the core and a PEG shell were synthesized by surfactant-free emulsion polymerization (SFEP) in sizes from 51 to 162 nm and PDI below 0.138, varying the PDEAEM content (17−40 wt %) using a 1 L reactor that allows nanogel preparation in gram quantities.

The cross-linker used in the preparation of nanogels has a significant impact on their properties:

- EGDMA yields nanogels that are very stable up to 18 months at room temperature. These nanogels swell at mildly acidic conditions and deliver curcumin inside colon cancer cell lines effectively.
- DVA yields acid-degradable nanogels (pH 6). These nanogels deliver curcumin and degrade concomitantly inside cells.
- BAC yields nanogels showing both acid and GSH degradation behavior, with 100% of degradation in the presence of 3 mM GSH within 0.5 h. These nanogels deliver curcumin and degrade concomitantly inside cells.
- FDAC yields fluorescent nanogels. These nanogels can be tracked inside cells by fluorescence microscopy.

The nanogels were loaded with curcumin, showing an acceleration of curcumin release at a pH of 5 (mimicking the pH of lysosomes) for nanogels cross-linked with EGDMA and DVA, and, in the case of nanogels cross-linked with BAC, the release was even faster at pH 5 with the addition of 10 mM GSH.

The cell viability of the human colon cancer cell line (HCT-116) in contact with curcumin-loaded nanogels showed that the IC_{50} was lowered from 5 to 1 μg/mL when curcumin was loaded inside DVA-cross-linked and BAC-cross-linked nanogels.

Preliminary acute toxicity studies in mice showed that empty EGDMA-cross-linked and BAC-cross-linked PDEAEM-core-PEG-shell nanogels were nontoxic up to concentrations of 40 mg/kg.

The nanoformulation consisting of curcumin loaded inside PDEAEM-core-PEG-shell nanogels cross-linked with DVA or BAC has excellent potential for colon cancer therapy.

4. EXPERIMENTAL SECTION

4.1. Materials. *N*,*N*-(Diethylamino)ethyl methacrylate (DEAEM, Sigma-Aldrich 99%) was purified by distillation under reduced pressure prior to use. Poly(ethylene glycol) methyl ether methacrylate (PEGMA, MW = 950 and 2000 g/mol, Sigma-Aldrich) and ethylene glycol dimethacrylate (EGDMA, Sigma-Aldrich 98%) were purified by passing through an inhibitor remover column for hydroquinones (Sigma-Aldrich). 3,9-Divinyl-2,4,8,10-tetra-oxaspiro [5.5] undecane (DVA, 98%), *N*,*N*′-bis(acryloyl) cystamine (BAC, 98%), O−O′ fluorescein diacrylate (FDAC, 98%), ammonium persulfate (APS, 98%), curcumin (CUR, ≥94% (curcuminoid content), ≥80% (Curcumin)), and Tween 80 (Polysorbate 80), all from Sigma-Aldrich, were used as received. Phosphate-buffered solutions were prepared at 0.05 M total concentration using sodium chloride (99.4%, Fermont), sodium phosphate dibasic (98%, Sigma-Aldrich), and potassium phosphate monobasic (≥98%, Sigma-Aldrich). Further, NaOH (1 N) and HCl (2 N) solutions were prepared using sodium hydroxide pellets (97.8%, Fermont) and concentrated hydrochloric acid (60%, Fermont), respectively. Distilled water (Sparkletts, CA) was used for dialysis procedures.

4.2. Methods. *4.2.1. Synthesis of PDEAEM-Core-PEG-Shell Nanogels.* PDEAEM-core-PEG-shell nanogels were prepared by scaling up 16 times a previously reported methodology (from 50 to 800 mL).[39] Briefly, all nanogels were prepared by a surfactant-free emulsion polymerization (SFEP) method using different ratios of DEAEM to PEGMA; EGDMA, BAC, DVA, and FDAC were tested as cross-linkers, and APS was used as a free-radical initiator. One of the representative procedures for the preparation of the core−shell nanogels is described: DEAEM (5.6 g, 30.2 mmol) was mixed with the proper amounts of PEGMA with a MW of 2000 g/mol (2.4 g, 1.2 mmol) and EGDMA cross-linker (0.1197 g, 1.776 mmol) and dissolved in 50 mL of deionized water at room temperature. The mixture was bubbled with nitrogen for 30 min, before starting the polymerization reaction. The

https://dx.doi.org/10.1021/acsomega.9b04390
ACS Omega 2020, 5, 9171−9184

reaction mixture was then poured inside a 1 L jacketed glass reactor (Syrris, model Atlas Potassium, Royston, U.K.) containing 750 mL of deionized water at 80 °C and vigorously stirred (500 rpm). The initiator APS (0.192 g, 0.904 mmol) was dissolved in 10 mL of deionized water, and it was added immediately to the reaction vessel to act as a thermal initiator. The polymerization process was allowed to continue for two different reaction times, 0.5 and 1 h, and was stopped by cooling. The quantities of starting materials and the cross-linkers were varied to produce nanogels of different characteristics (Table 1). The resulting dispersions were purified via dialysis (Spectra/Por dialysis membrane, MWCO: 12 000−14 000 Da) against purified water at pH 5 for 13 days for the nanogels cross-linked with EGDMA and FDAC, followed by one day against distilled water, and against distilled water for 14 days for the nanogels cross-linked with DVA and BAC; in all cases, the total water amount was changed every 12 h. The nanogels were isolated by freeze-drying; for this step, the nanogel dispersion in water was carefully collected and frozen at −4 °C and then placed into the drying chamber of a Labconco Freeze Dry System FreeZone 4.5 (Kansas City, MI), precooled at −52 °C. Freeze-drying was performed at a pressure of 0.02 mbar for 48 h. After being dried, the nanogels were stored inside a desiccator at room temperature until further use for re-dispersion and/or characterization. The naming of the nanogels used N for nanogels; E = EGDMA, B = BAC, D = DVA, and F = FDAC for different cross-linkers used; and a running number.

4.2.2. Characterization of Nanogels. The chemical composition of the PDEAEM-core-PEG-shell nanogels was quantified by ^{1}H NMR spectroscopy (Bruker AVANCE III HD NMR 400 MHz equipment, Billerica, MA) using deuterated chloroform ($CDCl_3$), and the chemical shifts are reported in ppm using tetramethylsilane (TMS) as the internal standard. The size distribution of the nanogels was obtained by dynamic light scattering (DLS) using a Zetasizer Nano ZS (ZEN3690; Malvern Instruments, Worcestershire, U.K.) equipped with a red laser of 630 nm. The angle of measurements was 90°. Dialyzed and redispersed samples were analyzed. The hydrodynamic diameter (D_h) and polydispersity index (PDI) were calculated using the Malvern Instruments dispersion technology software based on CONTIN analysis and the Stokes−Einstein equation for spheres; for D_h, the average value of three measurements is reported. For the temperature sensitivity determination, a trend method was used from 30 to 55 °C in two-degree steps, equilibrating for 240 s once the measurement temperature was attained; the transition temperature reported is the minimum value of the first derivative of the swelling ratio (Q) of the nanogels (eq 1) with respect to temperature.

$$Q = \frac{V_s}{V_o} = \left(\frac{D_{h,s}^3}{D_{h,o}^3}\right) \quad (1)$$

where V_s is the volume of the nanogel in the swollen state, V_o is the volume of the nanogel in the collapsed state, $D_{h,s}$ is the hydrodynamic diameter of the nanogels in the swollen state, and $D_{h,o}$ is the hydrodynamic diameter of the nanogels in the collapsed state; the collapsed state was taken as the state at the highest temperature measured. To study the pH sensitivity, measurements were carried out at 25 °C from pH 5 to 9 (using buffer solutions) and Q was calculated assuming that the collapsed state was achieved at pH 9. The ζ-potential was also measured using the same Zetasizer Nano ZS by laser doppler microelectrophoresis. Measurements were performed on folded capillary cells at 25 °C. Atomic force microscopy (AFM) images were obtained using an Agilent SPM 5100 (Agilent Technologies, Santa Clara, CA) equipped with a high-resolution scanner N9520A (10 μm × 10 μm). Dialyzed nanogels before drying were dropped on freshly cleaved mica surfaces and air-dried at room temperature for 48 h. Images were acquired in the intermittent contact mode using silicon cantilevers (Budget Sensors). Images were processed using the WSxM software. Micrographs were also acquired using an analytical transmission electron microscope. The samples were observed at 200 kV by TEM (JEOL JEM-2200FS, Tokyo, Japan), and most of the images were acquired in the scanning transmission electron microscopy (STEM) mode, using a bright-field (BF) and high-angle annular dark-field (HAADF) detector. A drop of nanogel solution with and without phosphotungstic acid (Sigma-Aldrich), used as a staining agent, was poured onto copper grids (400-mesh covered with holey carbon) and the samples soft-dried at 30 °C. In the case of nanogels containing CUR, no staining agent was used and micrographs were acquired using an analytical field emission scanning electron microscope (FESEM) (Jeol model JSM-7800F Prime (JEOL Ltd., Tokyo, Japan)) in the STEM mode. A drop of the sample was poured onto copper tape for microscopy, followed by drying at room temperature.

4.2.3. Degradation Studies of PDEAEM-Core-PEG-Shell Nanogels Cross-Linked with BAC or DVA. The degradation of PDEAEM-core-PEG-shell nanogels cross-linked with BAC was evaluated by DLS by measuring the size changes of nanogels in response to different concentrations of GSH (1.5, 3, 6, and 10 mM) in a dispersion (1.0 mg/mL) prepared in aqueous medium of pH 7.2 at 37 °C. The samples were stirred (250 rpm) for 60 min, and the size changes of PDEAEM-core-PEG-shell nanogels cross-linked with BAC were measured by DLS every 15 min. The degradability of the nanogels cross-linked with DVA at acidic conditions at 37 °C was studied according to a previous report.[46] To a nanogel dispersion at pH 7.4, a HCl (2 N) solution was added dropwise, decreasing the pH to pH 5. The size distributions were measured by DLS.

4.2.4. Stability of Empty Nanogels in Biological Mimicking Media. The colloidal stability of empty PDEAEM-core-PEG-shell nanogels was analyzed at 37 °C under slow stirring from 15 min to 24 h by dilution of the samples to a final concentration used in the *in vitro* studies (25 μg/mL) in biological mimicking media: cell culture medium (RPMI-1640) supplemented with 10% v/v fetal bovine serum (FBS heat-inactivated from Sigma-Aldrich, St. Louis, MO) and 1% antibiotic−antimycotic (10 000 units penicillin, 10 mg streptomycin, and 25 mg/mL amphotericin B per mL, Sigma-Aldrich). The same nanogels were also analyzed at 37 °C in buffer solution (pH 7.4) after 48 h. The evolution of the hydrodynamic diameter (D_h) was monitored by DLS, using the equipment described before, equilibrating at 37 °C for 10 min before analysis.

4.2.5. Storage Stability. The stability of the empty nanogels cross-linked with EGDMA was evaluated using nonlyophilized nanogel dispersions stored at room temperature (25 °C) and monitored by DLS every month up to 4 months. In one case, its integrity was verified (size, PDI) until 18 months of storage. The stability of the curcumin-loaded nanogels was evaluated with formulations of curcumin-loaded nanogels stored at 37 °C

https://dx.doi.org/10.1021/acsomega.9b04390
ACS Omega 2020, 5, 9171−9184

in the dark and analyzed by DLS at 5, 7, 15, and 20 days until 30 days after preparation.

4.2.6. Loading of Curcumin into the PDEAEM-Core-PEG-Shell Nanogels. A dispersion of 40 mg of PDEAEM-core-PEG-shell nanogels was prepared in 20 mL of distilled water under constant stirring for 48 h. Subsequently, CUR was added to the nanogel dispersion in the weight ratio of nanogel/CUR of 4:1, and then, ethanol was added dropwise up to a final concentration of ∼5% (v/v). The final mixture was stirred for 48 h at room temperature and protected from light, leaving the container open to allow the slow evaporation of ethanol. Afterward, the dispersion was centrifuged at 3000 rpm, for 60 min, to remove insoluble curcumin. The clear yellowish supernatant was carefully collected and frozen at −4 °C and then placed into the drying chamber of a Labconco Freeze Dry System FreeZone 4.5 (Kansas City, MI), precooled at −52 °C. Freeze-drying was performed at a pressure of 0.02 mbar for 24 h. The drug-loaded nanogels were dispersed in ethanol for the determination of curcumin content and analyzed spectrophotometrically using a UV−vis spectrophotometer Varian Cary 100 (Agilent Technologies, Santa Clara, CA) at a wavelength of 427 nm. The drug-loading capacity (DLC %) and drug-loading efficiency (DLE %) were determined using eqs 2 and 3, respectively.

$$\text{DLC}\ (\%) = \left(\frac{\text{MDng}}{\text{Mng} + \text{MDng}}\right) \times 100 \tag{2}$$

$$\text{DLE}\ (\%) = \left(\frac{\text{MDng}}{\text{MD}}\right) \times 100 \tag{3}$$

where MDng is the mass of the drug in the nanogels, Mng is the mass of nanogels, and MD mass of drug in feed.

4.2.7. In Vitro Release of Curcumin from PDEAEM-Core-PEG-Shell Nanogels. For the controlled release studies, 6 mg of the CUR-loaded material was dispersed in 3 mL of buffer solution (pH 7.4 or 5) and then added to a dialysis tube (Spectra/Por MWCO: 12−14 kDa, from Spectrum, Los Angeles, CA). The dialysis tube was introduced into 30 mL of release medium inside an amber flask containing a solution of Tween 80 (0.5% v/v) in the corresponding buffer solution. The flask was placed inside a shaking bath (Thermo Scientific Precision SWB 15) operating at 37 °C and a shaking speed of 110 rpm. Aliquots of the medium (3 mL) were taken out at different times and replaced with fresh medium (PBS/Tween 80, 0.5% v/v) at every sampling time. The released fraction of CUR was calculated from UV measurements at 427 nm and then quantified using a calibration curve prepared for CUR in PBS/Tween 80 (0.5%v/v).

4.2.8. Colon Cancer Cell Culture and Viability Tests. The human colorectal cancer cell line HCT-116 (carcinoma) was obtained from the American Type Culture Collection (ATCC, Manassas, VA). HCT-116 cells were cultivated at 37 °C with 5% CO_2 in RMPI-1640 medium supplemented with 10% v/v fetal bovine serum (FBS heat-inactivated from Sigma-Aldrich, St. Louis, MO) and 1% antibiotic−antimycotic (10 000 units penicillin, 10 mg streptomycin, and 25 mg/mL amphotericin B per mL, Sigma-Aldrich). Cells were grown to 75−85% confluence, detached with 0.25% trypsin−0.1% ethylenediaminetetraacetic acid (EDTA), and used for assay protocols.

Cell viability was determined using the *in vitro* MTT-based toxicology assay (Sigma-Aldrich). HCT-116 cells were seeded by triplicate in a 96-well plate (2.5×10^5 cells/well) and incubated under standard growth conditions for 24 h, followed by the addition of curcumin in various concentrations, PDEAEM-core-PEG-shell nanogels, and curcumin-loaded PDEAEM-core-PEG-shell nanogels. In all assays, untreated cells were used as the negative control (C−) and 5% DMSO as positive dead control (C+), and cells were incubated for 24 h. After treatment time, MTT solution (10 μL) was added to the cells for 4 h to form formazan crystals by mitochondrial dehydrogenases. Then, 100 μL of solubilization buffer (10% Triton X-100, 0.1 N HCl in anhydrous isopropanol) was added to each well and incubated at 37 °C with 5% CO_2 for 18 h to dissolve the formazan crystals, and the amount of formazan converted by viable cells was determined by measuring the absorbance at 570 nm on a 96-well microplate reader EPOCH (BioTek, Winooski, VT). The results were normalized to untreated cells (100%) to obtain the percentage of cell viability and expressed as the average ± standard error of the mean (SEM) of triplicates. Results were examined statistically by an unpaired Student's *t*-test. All statistical analyses were performed using the GraphPad prism program, version 5.0. Values of $^*p < 0.05$, $^{**}p < 0.01$, and $^{***}p < 0.001$ were considered statistically significant.

4.2.9. Cellular Uptake Studies by Fluorescence Microscopy. The cellular uptake of curcumin and nanogels was visualized using fluorescence microscopy. Cell images were obtained in an inverted microscope EVOS Floid Cell Imaging Station (Life Technologies, Carlsbad, CA) at 20× magnification. The samples were treated by two methodologies: (a) curcumin and CUR-loaded nanogel uptake and (b) empty nanogel uptake.

(a) HCT-116 cells were seeded in 96-well plates (Corning) and incubated for 24 h with PDEAEM-core-PEG-shell nanogels, curcumin-loaded PDEAEM-core-PEG-shell nanogels, and free curcumin (concentrations equivalent to 1 or 5 μg CUR/mL) at 37 °C with 5% CO_2. Plates were treated with 50 μg/mL propidium iodide (PI) (Sigma-Aldrich) and 10 μg/mL Hoechst 33258 and were incubated for 30 min before observations.

(b) HCT-116 cells were cultured in duplicate in a 96-well plate (5×10^3 cells/mL) using RPMI-1640 medium supplemented with 10% FBS at 37 °C and 5% CO_2 using a humidified incubator for 24 h. Afterward, fluorescent nanogels (NF1, Table 1) were added into each well at a concentration of 100 μg/mL and incubated at 37 °C for 0.5 h. Then, 100 μL of cold RPMI-1640 culture medium was added to stop the cellular uptake. HCT-116 cells were centrifuged at 400*g* (5 min), and the supernatant was removed. Next, cells were treated for 5 min with Hoechst 33258 on PBS 1× (pH 7.4, 1:1000) to stain the cell nuclei, washed once with PBS, and centrifuged at 400*g* (5 min). After treatments, the samples were exposed to red light (586-15/646-68 nm), blue light (390-40/446-33 nm), and green light (482-18/532-59 nm) on the fluorescence microscope. Each image was edited using the Image J software.

4.2.10. In Vivo Acute Toxicity Studies. 4.2.10.1. Animals. Female CD1 mice purchased from Circulo ADN (Mexico City, Mexico) with the weight between 16 and 20 g and 3−5 weeks old were used. Mice were kept in the Animal Care Systems Optimice with water and food ad libitum, light and dark cycles of 12 h, and temperature between 21 and 23 °C. All animal

https://dx.doi.org/10.1021/acsomega.9b04390
ACS Omega 2020, 5, 9171−9184

experiments were conducted following the guidelines of the guide Institute of Laboratory Animal Resources, National Research Council,[58] and approval of the Institute's ethical committee on animal experimentation (approval number CBE/PRES-O/011).

4.2.10.2. Determination of LD_{50} via the Intraperitoneal Route. The peritoneal cavity is a zone with the abundant blood supply that facilitates rapid absorption, usually one-half to one-quarter as rapid as that from the intravenous route, and is the most common route because it is technically simple and easy.[59] The experiments were performed in four groups. Each group received a different compound in doses ranging between 10 and 40 mg/kg, with a dose progression factor of 0.3 on a log scale. The upper limit in the dosage scheme is limited by the solubility of the compounds to form an aqueous solution. Nanogels in the lyophilized form were resuspended in injectable water by sonication for 20 min before injection. A stock solution at 4 mg/mL was prepared for each compound. From this stock solution, dilutions were prepared to achieve the desired concentrations. The volume of injection in all of the experiments was kept at 0.25 mL. Dixon's up-and-down method for estimation of median lethal dose (LD_{50}) was used to minimize the number of animals. According to this protocol, the first animal receives a lower dose than the best preliminary estimate of the LD_{50}. If the animal survives, it is represented as O, and the second animal receives a higher dose. If the first animal dies, it is represented as X, and the second animal receives a lower dose. The survival or death of each animal at a determined concentration decides whether the next dose must be increased or decreased.[60] The animals were observed for 48 h to determine each result. The experiment stops when one of the following criteria first is met: (a) Three consecutive animals survive at the upper bound; (b) five reversals occur in any six consecutive animals tested; and (c) at least four animals have followed the first reversal, and the specified likelihood ratios exceed the critical value.[57] As described in the OCED protocol,[57] the likelihood function for the estimation of LD_{50} is written as follows: $L = L_1, L_2, ..., L_n$. Here, L is the likelihood of the experimental outcome, given μ and σ, and n is the total number of animals tested. $L_i = 1 - F(Z_i)$ if the ith animal survives, or $L_i = F(Z_i)$ if the ith animal dies, where F is the cumulative standard normal distribution, $Z_i = [\log(d_i) - \mu]/\sigma$, d_i is the dose given to the ith animal, and σ is the standard deviation in log units of dose.

The individual weights of each animal were recorded before the dose and then for 10 days, as reported in the Supporting Information (SI) Tables S1 and S2.

■ ASSOCIATED CONTENT

Supporting Information

The Supporting Information is available free of charge at https://pubs.acs.org/doi/10.1021/acsomega.9b04390.

Scaled synthesis, DLS of nanogels listed in Table 1, ^{1}H NMR characterization, AFM images of nanogels, responsive behavior of PDEAEM-core-PEGMA-shell nanogels, degradation studies with GSH, scheme of acid degradation, stability of nanogels at different conditions, UV−vis calibration curves of CUR, FESEM image of a CUR-loaded PDEAEM-core-PEG-shell nanogel, fluorescence of CUR-loaded nanogels, stability of CUR-loaded nanogels, dose−response assay for empty nanogels into HCT-116, cytotoxic effect of empty degradable PDEAEM-core-PEG-shell nanogels, fluorescence microscope images of CUR and CUR-loaded PDEAEM-core-PEG-shell nanogels in contact with HCT-116 cells, and weight of mice during experiments (PDF)

■ AUTHOR INFORMATION

Corresponding Author

Angel Licea-Claverie − *Centro de Graduados e Investigación en Química, Instituto Tecnológico de Tijuana, Tijuana 22410, Baja California, México;* orcid.org/0000-0002-0725-0980; Phone: +52-664-6234043; Email: aliceac@tectijuana.mx

Authors

Lizbeth A. Manzanares-Guevara − *Centro de Graduados e Investigación en Química, Instituto Tecnológico de Tijuana, Tijuana 22410, Baja California, México*

Irasema Oroz-Parra − *Facultad de Ciencias Marinas, Universidad Autónoma de Baja California, Ensenada 22860, Baja California, México*

Johanna Bernaldez-Sarabia − *Departamento de Innovación Biomédica, Centro de Investigación Científica y de Educación Superior de Ensenada (CICESE), Ensenada 22860, Baja California, México*

Fernando Diaz-Castillo − *Departamento de Innovación Biomédica, Centro de Investigación Científica y de Educación Superior de Ensenada (CICESE), Ensenada 22860, Baja California, México*

Alexei F. Licea-Navarro − *Departamento de Innovación Biomédica, Centro de Investigación Científica y de Educación Superior de Ensenada (CICESE), Ensenada 22860, Baja California, México;* orcid.org/0000-0003-4022-7405

Complete contact information is available at: https://pubs.acs.org/10.1021/acsomega.9b04390

Author Contributions

The paper was written through contributions of all authors. All authors have given approval to the final version of the paper.

Notes

The authors declare no competing financial interest.

■ ACKNOWLEDGMENTS

We are grateful to Alejandro Ramirez (CGIQ, TNM/IT-Tijuana) for AFM images, Ignacio Rivero (CGIQ, TNM/IT-Tijuana) for FESEM images, and Francisco Paraguay (CIMAV-Chihuahua) for TEM images. Technical support by Valentin Miranda (CGIQ, TNM/IT-Tijuana) in NMR measurements and by Samanta M. Jimenez-Flores (CICESE) for in vivo toxicity studies is also gratefully acknowledged. This investigation was supported by the National Council of Science and Technology of Mexico (CONACYT) through grant CB2016-285419. L.A.M.-G. thanks CONACYT for a Ph.D. scholarship. Secondary elements of Scheme 1, Figure 4, and the graphical abstract were designed by Freepik Company and are freely available.

■ REFERENCES

(1) World Health Organization. Cancer Fact Sheet. WHO Media Centre, 2018. Available online at: http://www.who.int/mediacentre/factsheets/fs297/en/ (accessed Nov 27, 2019).

(2) Senapati, S.; Mahanta, A. K.; Kumar, S.; Maiti, P. Controlled drug delivery vehicles for cancer treatment and their performance. *Signal Transduction Targeted Ther.* **2018**, 3, 1−17.

(3) Colson, Y. L.; Grinstaff, M. W. Biologically Responsive Polymeric Nanoparticles for Drug Delivery. *Adv. Mater.* **2012**, *24*, 3878−3886.
(4) Oishi, M.; Nagasaki, Y. Stimuli-responsive smart nanogels for cancer diagnostics and therapy. *Nanomedicine* **2010**, *5*, 451−468.
(5) Maya, S.; Sarmento, B.; Nair, A.; Rejinold, N. S.; Nair, S. V.; Jayakumar, R. Smart stimuli sensitive Nanogels in Cancer drug delivery and imaging: a review. *Curr. Pharm. Des.* **2013**, *19*, 7203−7218.
(6) Liechty, W. B.; Peppas, N. A. Expert opinion: responsive polymer nanoparticles in cancer therapy. *Eur. J. Pharm. Biopharm.* **2012**, *80*, 241−246.
(7) Zha, L.; Banik, B.; Alexis, F. Stimulus responsive nanogels for drug delivery. *Soft Matter* **2011**, *7*, 5908−5916.
(8) Cuggino, J. C.; Osorio-Blanco, E. R.; Gugliotta, L. M.; Alvarez-Igarzabale, C. I.; Calderón, M. Crossing biological barriers with nanogels to improve drug delivery performance. *J. Controlled Release* **2019**, *307*, 221−246.
(9) Cuggino, J. C.; Gatti, G.; Picchio, M. L.; Maccioni, M.; Gugliotta, L. M.; Alvarez-Igarzabal, C. I. Dually responsive nanogels as smart carriers for improving the therapeutic index of doxorubicin for breast cancer. *Eur. Polym. J.* **2019**, *116*, 445−452.
(10) Soni, K. S.; Desale, S. S.; Bronich, T. K. Nanogels: an overview of properties, biomedical applications and obstacles to clinical translation. *J. Controlled Release* **2016**, *240*, 109−126.
(11) Eckmann, D. M.; Composto, R. J.; Tsourkas, A.; Muzykantov, V. R. Nanogel carrier design for targeted drug delivery. *J. Mater. Chem. B* **2014**, *2*, 8085−8097.
(12) Chiang, W. H.; Ho, V. T.; Huang, W. C.; Huang, Y. F.; Chern, C. S.; Chiu, H. C. Dual Stimuli-Responsive Polymeric Hollow Nanogels Designed as Carriers for Intracellular Triggered Drug Release. *Langmuir* **2012**, *28*, 15056−15064.
(13) Chiang, W. H.; Huang, W. C.; Chang, Y. J.; Shen, M. Y.; Chen, H. H.; Chern, C. S.; Chiu, H. C. Doxorubicin-Loaded Nanogel Assemblies with pH/Thermo-triggered Payload Release for Intracellular Drug Delivery. *Macromol. Chem. Phys.* **2014**, *215*, 1332−1341.
(14) Li, M.; Tang, Z.; Sun, H.; Ding, J.; Song, W.; Chen, X. pH and reduction dual-responsive nanogel cross-linked by quaternization reaction for enhanced cellular internalization and intracellular drug delivery. *Polym. Chem.* **2013**, *4*, 1199−1207.
(15) Rao, K. M.; Mallikarjuna, B.; Krishna-Rao, K. S. V.; Siraj, S.; Chowdoji, R. K.; Subha, M. C. S. Novel thermo/pH sensitive nanogels composed from poly(*N*-vinylcaprolactam) for controlled release of an anticancer drug. *Colloids Surf., B* **2013**, *102*, 891−897.
(16) Potinenia, A.; Lynn, D. M.; Langer, R.; Amiji, M. M. Poly(ethylene oxide)-modified poly(*β*-amino ester) nanoparticles as a pH-sensitive biodegradable system for paclitaxel delivery. *J. Controlled Release* **2003**, *86*, 223−234.
(17) Paramonov, S. E.; Bachelder, E. M.; Beaudette, T. T.; Standley, S. M.; Lee, C. C.; DasheJean, J.; Fréchet, M. J. Fully Acid-Degradable Biocompatible Polyacetal Microparticles for Drug Delivery. *Bioconjugate Chem.* **2008**, *19*, 911−919.
(18) Bachelder, E. M.; Beaudette, T. T.; Broaders, K. E.; Paramonov, S. E.; DasheJean, J.; Fréchet, M. J. Acid-Degradable Polyurethane Particles for Protein-Based Vaccines: Biological Evaluation and in Vitro Analysis of Particle Degradation Products. *Mol. Pharmaceutics* **2008**, *5*, 876−884.
(19) Schafer, F. Q.; Buettner, G. R. Redox environment of the cell as viewed through the redox state of the glutathione disulfide/glutathione couple. *Free Radical Biol. Med.* **2001**, *30*, 1191−1212.
(20) Wang, S.; Huang, P.; Chen, X. Y. Stimuli-responsive programmed specific targeting in nanomedicine. *ACS Nano* **2016**, *10*, 2991−2994.
(21) Ye, M. X.; Li, Y.; Yin, H.; Zhang, J. Curcumin: updated molecular mechanisms and intervention targets in human lung cancer. *Int. J. Mol. Sci.* **2012**, *13*, 3959−3978.
(22) Duvoix, A.; Blasius, R.; Delhalle, S.; et al. Chemopreventive and therapeutic effects of curcumin. *Cancer Lett.* **2005**, *223*, 181−190.
(23) Devassy, J. G.; Nwachukwu, I. D.; Jones, P. J. Curcumin and cancer: barriers to obtaining a health claim. *Nutr. Rev.* **2015**, *73*, 155−165.
(24) Guilford, J. M.; Pezzuto, J. M. Natural products as inhibitors of carcinogenesis. *Expert Opin. Invest. Drugs* **2008**, *17*, 1341−1352.
(25) Aggarwal, B. B.; Sundaram, C.; Malani, N.; Ichikawa, H. Curcumin: the Indian solid gold. *Adv. Exp. Med. Biol.* **2007**, *595*, 1−75.
(26) Singh, S. From exotic spice to modern drug? *Cell* **2007**, *130*, 765−768.
(27) Alpers, D. H. The potential use of curcumin in management of chronic disease: too good to be true? *Curr. Opin. Gastroenterol.* **2008**, *24*, 173−175.
(28) Chen, A.; Xu, J.; Johnson, A. C. Curcumin inhibits human colon cancer cell growth by suppressing gene expression of epidermal growth factor receptor through reducing the activity of the transcription factor Egr-1. *Oncogene* **2006**, *25*, 278−287.
(29) Anand, P.; Kunnumakkara, A. B.; Newman, R. A.; Aggarwal, B. B. Bioavailability of curcumin: problems and promises. *Mol. Pharm.* **2007**, *4*, 807−818.
(30) Aggarwal, B. B.; Sung, B. Pharmacological basis for the role of curcumin in chronic diseases: an age-old spice with modern targets. *Trends Pharmacol. Sci.* **2009**, *30*, 85−94.
(31) Cheng, A.-L.; Hsu, C. H.; Lin, J. K.; Hsu, M. M.; Ho, Y. F.; Shen, T. S. Phase I clinical trial of curcumin, a chemopreventive agent, in patients with high-risk or premalignant lesions. *Anticancer Res.* **2001**, *21*, 2895−2900.
(32) Torchilin, V. Multifunctional and stimuli-sensitive pharmaceutical nanocarriers. *Eur. J. Pharm. Biopharm.* **2009**, *71*, 431−444.
(33) Lee, W. H.; Loo, C. Y.; Young, P. M.; Traini, D.; Mason, R. S.; Rohanizadeh, R. Recent advances in curcumin nanoformulation for cancer therapy. *Expert Opin. Drug Delivery* **2014**, *11*, 1183−1201.
(34) Bose, S.; Panda, A. K.; Mukherjee, S.; Sa, G. Curcumin and tumor immune-editing: resurrecting the immune system. *Cell Div.* **2015**, *10*, 1−13.
(35) Yallapu, M. M.; Nagesh, P. K.; Jaggi, M.; Chauhan, S. C. Therapeutic applications of curcumin nanoformulations. *AAPS J.* **2015**, *17*, 1341−1356.
(36) Rao, K. M.; Krishna Rao, K. S.; Ramanjaneyulu, G.; Ha, C. S. Curcumin encapsulated pH sensitive gelatin based interpenetrating polymeric network nanogels for anti-cancer drug delivery. *Int. J. Pharm.* **2015**, *478*, 788−795.
(37) Rana, V.; Sharma, R. *Applications of Targeted Nano Drugs and Delivery Systems*; Mohapatra, S. S.; Ranjan, S.; Dasgupta, N.; Mishra, R. K.; Thomas, S., Eds.; Elsevier: New York, 2019; Chapter 5, pp 93−131.
(38) Owens, D. E., III; Peppas, N. A. Opsonization, biodistribution, and pharmacokinetics of polymeric nanoparticles. *Int. J. Pharm.* **2006**, *307*, 93−102.
(39) Manzanares-Guevara, L. A.; Licea-Claverie, A.; Paraguay-Delgado, F. Preparation of stimuli responsive nanogels based on poly(N,N-diethylaminoethyl methacrylate) by a simple "surfactant-free" methodology. *Soft Mater.* **2018**, *16*, 37−50.
(40) Pikabea, A.; Aguirre, J.; Miranda, J. I.; Ramos, J.; Forcada, J. Understanding of Nanogels Swelling Behavior Through a Deep Insight into Their Morphology. *J. Polym. Sci., Part A: Polym. Chem.* **2015**, *53*, 2017−2025.
(41) Obeso-Vera, C.; Cornejo-Bravo, J. M.; Serrano-Medina, A.; Licea-Claverie, A. Effect of crosslinkers on size and temperature sensitivity of poly(*N*-isopropylacrylamide) microgels. *Polym. Bull.* **2013**, *70*, 653−664.
(42) Pikabea, A.; Ramos, J.; Forcada, J. Production of cationic nanogels with potential use in controlled drug delivery. *Part. Part. Syst. Charact.* **2014**, *31*, 101−109.
(43) Marek, S. R.; Coon, C. A.; Peppas, N. A. Cationic Nanogels Based On Diethylaminoethyl Methacrylate. *Polymer* **2010**, *51*, 1237−1243.

https://dx.doi.org/10.1021/acsomega.9b04390
ACS Omega 2020, 5, 9171−9184

(44) Hayashi, H.; Iijima, M.; Kataoka, K.; Nagasaki, Y. pH-Sensitive Nanogel Possessing Reactive PEG Tethered Chains on the Surface. *Macromolecules* **2004**, *37*, 5389−5396.
(45) Kumar, P.; Liu, B.; Behl, G. A Comprehensive Outlook of Synthetic Strategies and Applications of Redox-Responsive Nanogels in Drug Delivery. *Macromol. Biosci.* **2019**, *19*, No. 1900071.
(46) Manzanares-Guevara, L. A.; Licea-Claverie, A.; Oroz-Parra, I.; Licea-Navarro, A. F. On the cytotoxicity of a cationic tertiary amine PEGylated nanogel as nanocarrier for anticancer therapies. *MRS Commun.* **2018**, *8*, 1204−1210.
(47) Peng, H.; Huang, X.; Melle, A.; Karperien, M.; Pich, A. Redox-responsive degradable prodrug nanogels for intracellular drug delivery by crosslinking of amine-functionalized poly(*N*-vinylpyrrolidone) copolymers. *J. Colloid Interface Sci.* **2019**, *540*, 612−622.
(48) Nuhn, L.; Gietzen, S.; Mohr, K.; Fischer, K.; Toh, K.; Miyata, K.; Matsumoto, Y.; Kataoka, K.; Schmidt, M.; Zentel, R. Aggregation Behavior of Cationic Nanohydrogel Particles in Human Blood Serum. *Biomacromolecules* **2014**, *15*, 1526−1533.
(49) Lee, P. Y.; Tuan-Mu, H. Y.; Hsiao, L. W.; Hu, J. J.; Jan, J. S. Nanogels comprising reduction-cleavable polymers for glutathione-induced intracellular curcumin delivery. *J. Polym. Res.* **2017**, *24*, No. 66.
(50) Wu, W.; Shen, J.; Banerjee, P.; Zhou, S. Water-dispersible multifunctional hybrid nanogels for combined curcumin and photothermal therapy. *Biomaterials* **2011**, *32*, 598−609.
(51) Zhu, W. T.; Liu, S.; Wu, L.; Xu, H.; Wang, J.; Ni, G.; Zeng, Q. Delivery of curcumin by directed self-assembled micelles enhances therapeutic treatment of non-small-cell lung cancer. *Int. J. Nanomedicine* **2017**, *12*, 2621−2634.
(52) He, C.; Hua, Y.; Yin, L.; Tang, C.; Yin, C. Effects of particle size and surface charge on cellular uptake and biodistribution of polymeric nanoparticles. *Biomaterials* **2010**, *31*, 3657−3666.
(53) Gao, H.; Shi, W.; Freund, L. B. Mechanics of receptor-mediated endocytosis. *Proc. Natl. Acad. Sci. U.S.A.* **2005**, *102*, 9469−9474.
(54) Oishi, M.; Hayashi, H.; Iijimad, M.; Nagasaki, Y. Endosomal release and intracellular delivery of anticancer drugs using pH-sensitive PEGylated nanogels. *J. Mater. Chem.* **2007**, *17*, 3720−3725.
(55) Liechty, W. B.; Scheuerle, R. L.; Vela-Ramirez, J. E.; Peppas, N. A. Uptake and function of membrane-destabilizing cationic nanogels for intracellular drug delivery. *Bioeng. Transl. Med.* **2019**, *4*, 17−29.
(56) Gonzalez-Urias, A.; Zapata-Gonzalez, I.; Licea-Claverie, A.; Licea-Navarro, A. F.; Bernaldez-Sarabia, J.; Cervantes-Luevano, K. Cationic versus anionic core-shell nanogels for transport of cisplatin to lung cancer cells. *Colloids Surf., B.* **2019**, *182*, No. 110365.
(57) OECD. *Test No. 425: Acute Oral Toxicity: Up-and-Down Procedure, OECD Guidelines for the Testing of Chemicals, Section 4*; OECD Publishing: Paris, 2008. https://doi.org/10.1787/9789264071049-en.
(58) Committee for the Update of the Guide for the Care and Use of Laboratory Animals. In *Guide for the Care and Use of Laboratory Animals*, 8th ed.; National Research Council (US), 2011.
(59) Jiro, H.; Shimizu, S. Routes of Administration. In *The Laboratory Mouse*; Hedrich, H. J., Ed.; Elsevier: New York, 2012; Chapter 5.2, pp 709−725.
(60) Dixon, W. J. The Up-and-Down Method for Small Samples. *J. Am. Stat. Assoc.* **1965**, *60*, 967−978.

https://dx.doi.org/10.1021/acsomega.9b04390
ACS Omega 2020, 5, 9171−9184